We are IntechOpen,
the world's leading publisher of
Open Access books
Built by scientists, for scientists

6,900
Open access books available

186,000
International authors and editors

200M
Downloads

154
Countries delivered to

Our authors are among the

TOP 1%
most cited scientists

12.2%
Contributors from top 500 universities

WEB OF SCIENCE™

Selection of our books indexed in the Book Citation Index
in Web of Science™ Core Collection (BKCI)

Interested in publishing with us?
Contact book.department@intechopen.com

Numbers displayed above are based on latest data collected.
For more information visit www.intechopen.com

Chapter

Twist Tetrahedral-Tilting Structure Built from Photoluminescent Cadmium Chalcogenide Clusters

Wen-Chia Wu, Chung-Sung Yang and Yan Xu

Abstract

The newly synthesized cadmium chalcogenide ternary cluster is composed by six $[S_3Se]^{2-}$ tetrahedron units, coordinated with six Cd^{2+} cations. The potential cavity, calculated by the PLATON program, occupied 38.1% of crystal cell volume. The charge of unit cell is neutral. Therefore, the unit cell formula is determinate as $[Cd_6S_{18}Se_6]$. Two strong solid-state luminescence peaks, centered at 450 nm and 498 nm, were observed from the ternary $[Cd_6S_{18}Se_6]$ clusters by λ = 370 nm radiation. The 450 nm peak is due to the porosity property of cadmium chalcogenide clusters. However, the 498 nm peak has not been reported for the cadmium chalcogenide clusters before. In this study, we demonstrate that the 498 nm peak is attributed to the embedded Se atoms confined in the $[S3Se]^{2-}$ unit of $[Cd_6S_{18}Se_6]$ cluster. The luminescent output from the ternary $[Cd_8S_{18}Se_6]$ cluster is stable in room temperature for more than 6 months.

Keywords: cadmium chalcogenides, luminescence, porosity, quantum confinement

1. Introduction

For the past decade, an intensive interest has been shown in the area of developing porous optical supertetrahedral clusters, such as for selenides [1–5]. The direct assembly of chalcogenides into the cluster framework will be a benefit approach in the development of crystalline porous chalcogenides. Recently, the Tn supertetrahedral clusters [2–4] dominate the advantages in the field for using porous materials in luminescence application. The reason is that the larger size of the Tn supertetrahedral clusters usually leads to a highly open frame work with porosity higher than 50% [1, 5, 6]. Such a property is suitable for studying optoelectronic properties induced by the quantum size cluster.

Another famous porous structure, the perovskite clusters with R3C space group, is known for its ternary ABX_3 crystal structure as a light absorbent to be used in the solar cell area [7–9]. The porous spheres of perovskite $SrTiO_3$ spheres present superior performance in photocatalytic oxygen evolution [10]. The porous structure existed in the R3C type structure could be envisioned as an alternating choice to study the optoelectronic properties due to quantum confinement. To date, the use of existed porosity in R3C structure for quantum size luminescence application

is very rare [11]. Here, we employ the $Cd(SC_6H_4Me-4)_2$ as the starting material to prepare a novel ternary cadmium chalcogenide cluster $[Cd_6S_{18}Se_6]$ for studying the effect of crystalline porous frameworks in quantum size luminescence. The $[Cd_6S_{18}Se_6]$ cluster is potentially with porous R3C structure. The simpler atomic composition of R3C structure apparently allows one to manipulate the replaced site with more flexibility. Such an opportunity cannot be easily obtained from the larger Tn clusters [1, 4]. Thus, these ternary clusters will be more applicable in the study of the optoelectronic luminescent phenomena created by the embedded hetero-atoms (i.e., Se) in the quantum size cluster. Therefore, the quantum confinement luminescence induced by the Se atom confined in $[S_3Se]^{2-}$ tetrahedron is able to be observed in the ternary $[Cd_6S_{18}Se_6]$ cluster.

2. Experimental

The starting material, $Cd(SC_6H_4Me-4)_2$, was prepared according to reference [12]. The product is white precipitate with yield up to 75% in weight. The typical target cadmium chalcogenides compound, denoted as NCYU-6, was prepared as follows. $Cd(SC_6H_4Me-4)_2$ (100 mg), thiourea powder (50 mg, 99%, Alfa Aesar), tettrahydrofuran (4.5 mL, 99.9%, Pharmco), selenium powder (10 mg, 99.5%, Acros), and de-ionized H_2O (2.1 mL) were dissolved in a 33 mL stainless steel autoclave with lined Teflon. The reactants were stirred for 60 min before the sealed vessel was heated at 85°C for 28 days. When the reaction is finished, the autoclave was cooled down to room temperature for several hours in atmosphere. The product was then washed by a mixture of ethanol and methanol several times to remove any residue on crystals. The crystal is pale yellow and is stable in air, water, or polar solvents for several months. The yield is generally below 30% in weight. It is worthy to note that the weight ratio between Se and S should be carried out very precisely. If the derivation of Se/S weight ratio is higher than ±5%, no crystal could be found in the final product. For the experimental purpose, a yellow crystal, NCYU-7, was prepared via the same route as that of NCYU-6, except the addition of selenium powder in the reactants. The yield of NCYU-7 is ~50% in weight.

3. Result and discussion

The scanning electron microscopy (SEM) image of NCYU-6 is shown in **Figure 1(a)**. The geometry of NCYU-6 is tetragonal. The qualitative energy dispersive X-ray (EDX) spectrum, **Figure 1(b)**, confirms the existence of Cd (Lα = 3.13 eV, Lβ = 3.528 eV), S (Kα = 2.31 eV), and Se (L α = 1.388 eV) in NCYU-6. The geometry of NCYU-7 is similar to NCYU-7. The EDX spectrum shows that the Se peak is lack of in NCYU-7. Crystallographic structures were solved via single-crystal X-ray diffraction. Data were collected at room temperature on a SMART CCD diffractometer with Mo-Kα radiation. All framework atoms can be determined and a brief crystal data of NCYU-6 is given in **Table 1**. The most unique structure in NCYU-6 is the $[S_3Se]$ tetragon that is built up by three corner sulfur sites and one center Se site. Each corner sulfur site is bonded to two Cd atoms, two S atoms of tetragon, and the center Se atom. By using the bond valence sum theory [13], the bond order between corner S site and center Se site is 4/3. The bond order between S and S is 1/3. The local structure illustration of $[S_3Se]$ tetragon moiety is given in **Figure 2(a)**. On the other hand, the Cd atom is coordinated with six S atoms of $[S_3Se]^{2-}$ tetrahedron units for charge balance. Each $[S_3Se]$ tetragon is twisted 180° with adjacent $[S_3Se]^{2-}$ tetragon. The bond order between S site and
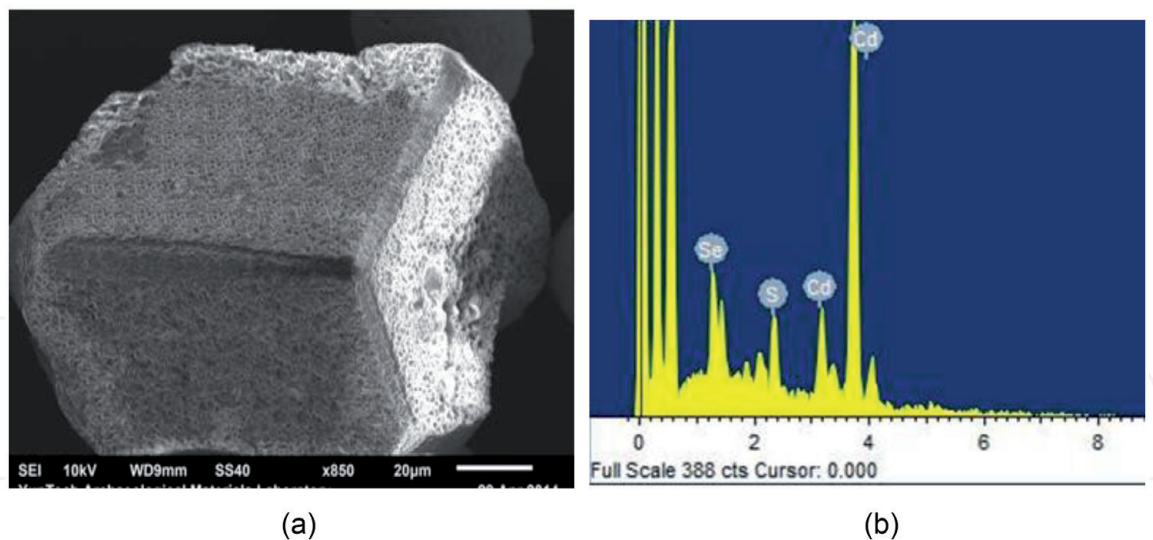
(a)   (b)

Figure 1.
(a) The SEM image of NCYU-6. The geometry of NCYU-6 is tetragonal. (b) the X-ray EDX spectrum confirms the existence of Cd (Lα = 3.13 eV, Lβ = 3.528 eV), S (Kα = 2.31 eV), and Se (L α = 1.388 eV) in NCYU-6.

Name	NCYU-6
Empirical formula	$Cd_6S_{18}Se_6$
Formula weight	1490.74
Temperature	295(2) K
Crystal system	Trigonal
Space group	R-3c
Unit cell dimensions	a = 4.9727(5) Å, α = 90°
	b = 4.9727(5) Å, β = 90°
	c = 16.981(3) Å, γ = 120°
Volume	363.64(9) Å^3
Z	1
Density (calculated)	6.807 Mg/m^3
Crystal size	0.05 × 0.03 × 0.03 mm^3
Reflections collected	949
Independent reflections	104 [R(int) = 0.0964]
Goodness-of-fit on F^2	1.331
Final R indices [I > 2sigma(I)]	R1 = 0.0735, wR2 = 0.2331
R indices (all data)	R1 = 0.0739, wR2 = 0.2344

Table 1.
Summary of crystal data and refinement for NCYU-6.

Cd site is assigned as 1/3. The local structure illustration of Cd atom coordinated with six S atoms of $[S_3Se]^{2-}$ units is given in **Figure 2(b)**. In the determination of Se location, the refined bond length data are used to verify the Se locations obtained from the R(F) value method. The bond lengths for six Cd-S locations are varied from 2.3476 Å to 2.3498 Å. The bond length of S_{1a} to center atom site (1.281 Å) is larger than the covalent radius of Se (1.16 Å) or (1.02 Å) [14]. Under the circumstance, replacement of the center site from S to Se is allowed by the architecture of
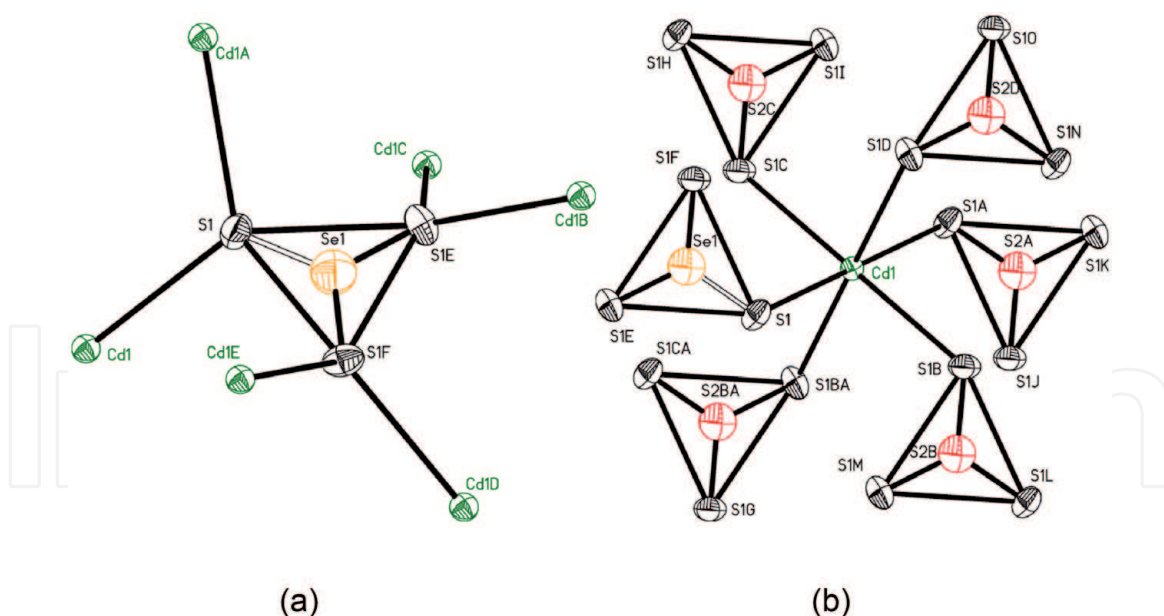
Figure 2.
(a) The local structure illustration of [S₃Se] tetragon moiety. The center site is marked with tangerine ball for Se atom. (b) the local structure illustration of Cd atom coordinated with six [S₃Se]²⁻ units. One [S₃Se] tetragon is shown to compare the size of thermal ellipsoids in ORTEP between S and Se. If the other five center S sites are replaced by Se, the R(F)ₐₗₗ ᵈₐₜₐ slightly increases from 5.27 to 7.39%.

tetragon, as shown in **Figure 2(a)**. During the crystallography determination for the location of Se, we found that the refined R(F) value is only slightly increased by an arbitrarily replacement of the center site of tetragon from S to Se atoms. For example, $R(F)_{all\ data}$ = 7.39% for [$Cd_6S_{18}Se_6$] and 5.27% for [Cd_6S_{24}]. Nevertheless, the arbitrarily replacement of the corner S site of tetragon by Se atom will make the R(F) value increase more than 60%, $R(F)_{all\ data}$ ~ 11.73%. Moreover, the size of thermal ellipsoids in ORTEP for the bridging location with Cd will increase to unreasonably large size. It is clear that the bridging location occupied by S atom is reasonable [1]. On the contrary, the size of thermal ellipsoids in ORTEP for the center site in tetragon is smaller, in comparison with the other corner S sites [1]. The center site occupied by Se atom is probable. The calculated occupancy possibility of the center site for Se to S is about ~80%. The occupancy possibility of the bridging site in tetragon cluster for Se to S is about ~20%. The temperature is an important factor in the refinement of S and Se locations. The results suggest that the center site of tetragon may have an affinity for Se atom and the hetero-atom substitution leads the new tetragonal-title architecture stable.

The atomic ratio for the NCYU-6 and NCYU-7 clusters was determined by the EDX spectrum qualitatively and the ICP-MS quantitatively. The quantitative elemental microanalysis of Cd/S for NCYU-7 is about 6:24 that is consistent with the composition and structure assignment by the crystallography. As for NCYU-6, the ratio of Se/S is analyzed as a function of the atom ratio (Se/S) of Se and S by ICP-MS. Four samples are prepared for the element concentration analysis for S and Se. The 5% HNO3 solution is employed to dissolve nine single crystals for the first and second ICP-MS measurements. As for the third, and forth measurements, 12 single crystals are picked up, respectively. The quantitative microanalysis data, provided in **Table 2,** show that the atomic ratio of Se (108 ppb) to S (335 ppb) in NCYU-6 is ~32.3%, i.e., Se/S ~ 1:3. By the combination of the data obtained from the above experiments, the unit cell formula is determined as [$Cd_6S_{18}Se_6$] for NCYU-6 (**Figure 3**). The unit cell formula for NCYU-7 is [Cd_6S_{24}].

The porosity data of the NCYU-6 were calculated by the PLATON crystallographic program, a versatile SHELX97 compatible multipurpose crystallographic

Wavelength	S = 180.771 nm		Se = 196.126 nm	
Sample_Name	Cc (ppb)	RSD (%)	Cc (ppb)	RSD (%)
1	351	2.2	117	2.8
2	347	1.1	118	2.9
3	326	0.9	103	1.5
4	326	0.9	102	1.5
Avg	337		108	

Table 2.
Summary of ICP-MS data of S and Se concentration in NCYU-6.
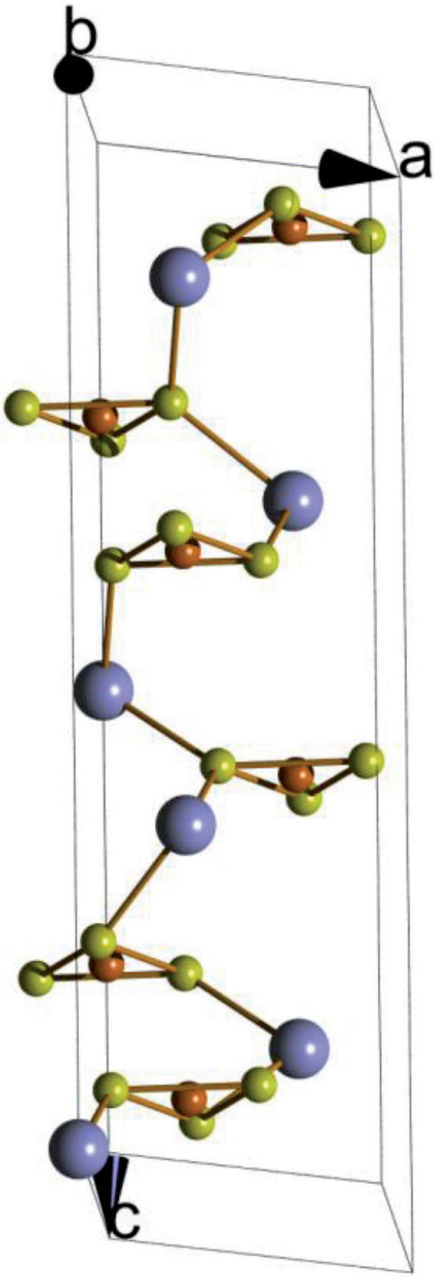
Figure 3.
The unit cell formula is determined as [$Cd_6S_{18}Se_6$] for NCYU-6. The blue ball stands for Cd atom. Dark yellow ball stands for S atom. Tangerine ball stands for Se atom.

toolkit software program [15]. In per unit cell of NCYU-6 (363.64 Å^3), the volume occupied by solvent is 138.5Å^3. The potential cavity occupied 38.1% of crystal cell volume. The percentage of cavity derived from NCYU-6 suggests that considerable
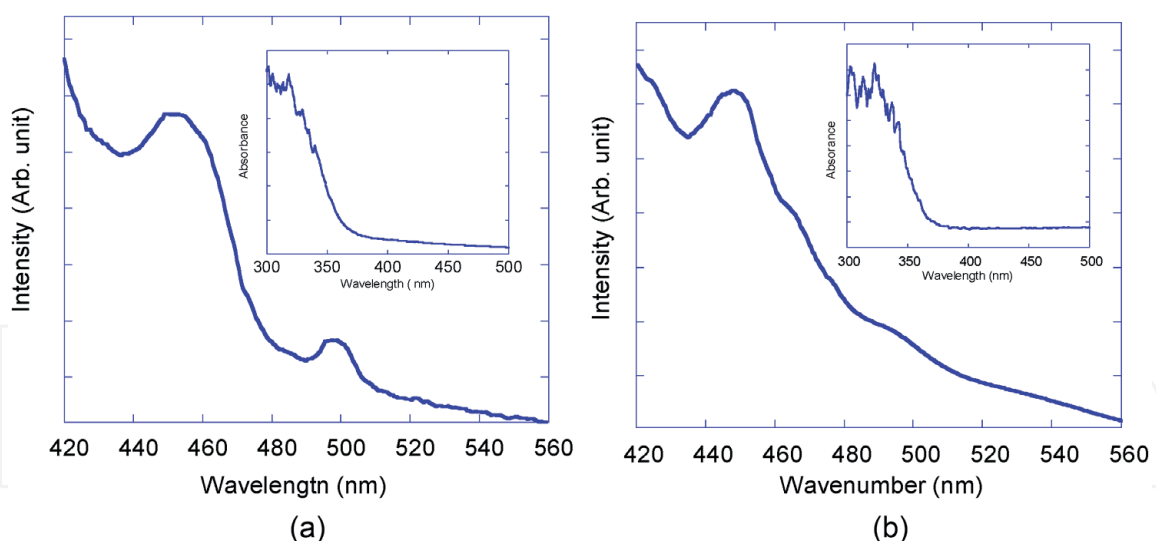
Figure 4.
Solid-state PL spectra were excited at 370 nm at RT. (a) Two emission peaks, centered at 450 nm and 498 nm, are revealed from NCYU-6. (b) Only one peak (450 nm) is observed from NCYU-7. The inset figures are DRS spectra for NCYU-6 and NCYU-7, respectively.

amount of guest molecules, i.e., tetrahydrofuran, presents in the structure of open framework. The guest molecules possibly occupied two domains to make this material with porosity. The possible domains are the in-plane pore window and the space between layers. Since the framework of the layer is wavy, the distance between layers is flexible and is adjustable by the template.

The UV–vis diffuse reflectance spectrum (DRS) of NCYU-6 and NCYU-7 are given in inset of **Figure 4(a)** and **(b)**, respectively. The bandgap of the NCYU-6 is 390 nm (3.14 eV) is 380 nm (3.26 eV) for NCYU-7. The suitable bandgaps make these two compounds possible to be used in photocatalytic reaction of hydrogen generation under UV and visible blue light irradiation [16–18].

Solid-state photoluminescence spectra (PL) were carried on Hitachi F-2500 fluorescence spectrophotometer. The emission spectra were excited at 370 nm at room temperature (RT). In the RT spectra, two emission peaks, centered at about 450 nm and 498 nm, are revealed from NCYU-6, and only one peak (450 nm) is observed for NCYU-7 (**Figure 4(a)** and **(b)**). The peak at 450 nm is generally attributed to the porosity property of open framework [1, 5]. The porosity created by the tilt-tetragonal structure allows the insertion of organic template molecule, tetrtahydrofuran [1, 5]. Thus, the conversion of UV radiation (370 nm) to visible violet light, ~450 nm, is possible. The reason is that the emission peak is induced by the interaction between the inorganic and organic phosphors [19, 20]. So far, the 498 nm emission peak has not been reported for the title-tetragonal R-3c structure before. The replacement of S atom(s) by Se atom(s) in the NCYU-6 is expected to output an absorption peak due to the quantum confinement of Se atom(s) [1, 5]. More experimental data are needed to explore the shift mechanism of the PL peak. However, it is believed that the red-shifted band-edge emission (P-type dopant) is relevant with the center site of Se atoms in tilt-tetragonal R−3c structure.

4. Conclusion

The novel ternary $[Cd_6S_{18}Se_6]$ cluster is prepared via a hydrothermal method. The space group of $[Cd_6S_{18}Se_6]$ is R3C. The six $[S_3Se]$ tetragon units of $[Cd_6S_{18}Se_6]$ are twisted 180 degree with each other. The cavity occupied 38.1% of $[Cd_6S_{18}Se_6]$ crystal cell volume. In the solid-state PL spectra, the peak centered at 450 nm

is induced by the porosity property of cadmium chalcogenides clusters, i.e., the interaction between the inorganic and organic phosphors inside the cavity of unit cell. The peak located at 498 nm is due to the quantum confinement of Se atom(s) in [S_3Se] tetragon unit.

Acknowledgements

Author details

Wen-Chia Wu[1], Chung-Sung Yang[1]* and Yan Xu[2]

1 Department of Applied Chemistry, National Chia Yi University, Chiayi, Taiwan, ROC

2 Department of Applied Chemistry, Northwest A&F University, Xianyang, Shanxi, People's Republic of China

*Address all correspondence to: csyang@mail.ncyu.edu.tw

IntechOpen

References

[1] Chen C-J, Yang C-S, Lin X-H. Synthesis, characterization, and photoluminescence of quaternary [Cd4In16S33 – xSex]10– supertetrahedral clusters: (0.33 < x < 0.45). Inorganic Chemistry Communications. 2005;**8**:836-840

[2] Li H, Laine A, O'Keeffe M, Yaghi OM. Supertetrahedral sulfide crystals with giant cavities and channels. Science. 1999;**1999**(283):1145-1147

[3] Bu X, Zheng N, Wang X, Wang B, Feng P. Three-dimensional frameworks of gallium selenide supertetrahedral clusters. Angewandte Chemie, International Edition. 2004;**43**:1502-1505

[4] Wang C, Lin Y, Bu X, Zheng N, Zivkovic O, Yang C-S, et al. Three-dimensional superlattices built from (M4In16S33)10- (M = Mn, Co, Zn, Cd) supertetrahedral clusters. Journal of the American Chemical Society. 2001;**123**:11506-11507

[5] Chen C-Y, Ou C-C, Huang H-F, Cheng J-H, Yang C-S. Mixed pentasupertetrahedral P1 and supertetrahedral T2 clusters as building units to create two-dimensional indium chalcogenides open framework. Inorganic Chemistry Communications. 2011;**14**:1004-1009

[6] Bu X, Zheng N, Li Y, Feng P. Pushing up the size limit of chalcogenide supertetrahedral clusters: Two- and three-dimensional photoluminescent open frameworks from $(Cu_5In_{30}S_{54})^{13-}$ clusters. Journal of the American Chemical Society. 2002;**124**:12646-12467

[7] Baikie T, Fang Y, Kadro JM, Schreyer MK, Wei F, Mhaisalkar SG, et al. Synthesis and crystal chemistry of the hybrid perovskite (CH_3NH_3) PbI_3 for solid-state sensitised solar cell applications. Journal of Materials Chemistry A. 2013;**1**:5628-5641

[8] Kim HS, Lee JW, Yantara N, Boix PP, Kulkarni SA, Mhaisalkar S, et al. High efficiency solid-state sensitized solar cell-based on submicrometer rutile TiO_2 nanorod and $CH_3NH_3PbI_3$ perovskite sensitizer. Nano Letters. 2013;**13**:2412-2417

[9] Burschka J, Pellet N, Moon S-J, Humphry-Baker R, Gao P, Nazeeruddin MK, et al. Sequential deposition as a route to high-performance perovskite-sensitized solar cells. Nature. 2013;**499**:316-319

[10] Pan JH, Shen C, Ivanova I, Zhou N, Wang X, Tan WC, et al. Self-template synthesis of porous perovskite titanate solid and hollow submicrospheres for photocatalytic oxygen evolution and mesoscopic solar cells. ACS Applied Materials & Interfaces. 2015;**7**:14859-14869

[11] Sichert JA, Tong Y, Mutz N, Vollmer M, Fischer S, Milowska KZ, et al. Quantum size effect in organometal halide perovskite nanoplatelets. Nano Letters. 2015;**15**:6521-6527

[12] Dance I, Garbutt RG, Craig DC, Scudder ML. The different nonmolecular polyadamantanoid crystal structures of cadmium benzenethiolate and 4-methylbenzenethiolate. Analogies with microporous aluminosilicate frameworks. Inorganic Chemistry. 1987;**26**:4057-4064

[13] Altermatt D, Brown ID. Bond-valence parameters obtained from a systematic analysis of the inorganic crystal structure database. Acta Crystallographica. Section B. 1985;**41**:244-247

[14] Data adopted from Cambridge Structural Database (CSD)

[15] Speck AL. Single-crystal structure validation with the program PLATON. Journal of Applied Crystallography. 2003;**36**:7-13

[16] Ou C-C, Yang C-S, Lin S-H. Selective photo-degradation of Rhodamine B over zirconia incorporated titania nanoparticles: A quantitative approach. Catalysis Science & Technology. 2011;**1**:295-307

[17] Lin S-H, Ou C-C, Su MD, Yang C-S. Photo-catalytic behavior of vanadia incorporated titania nanoparticles. Catalysis Science & Technology. 2013;**3**:2081-2091

[18] Chang Y-H, Ou C-C, Yeh H-W, Yang C-S. Photo-catalytic selectivity of anthranilic acid over iron oxide incorporated titania nanoparticles: Influence of the Fe_2+/Fe_3+ ratio of iron oxide. Journal of Molecular Catalysis A: Chemical. 2016;**412**:67-77

[19] Feng P. Photoluminescence of open-framework phosphates and germanates. Chemical Communications. 2001:1668-1669

[20] Xu X, Wang W, Liu D, Hu D, Wu T, Bu X, et al. Pushing up the size limit of metal chalcogenide supertetrahedral nanocluster. Journal of the American Chemical Society. 2018;**140**:888-891